

GroEL Channels the Folding of Thioredoxin Along One Kinetic Route

Nidhi Bhutani and Jayant B. Udgaonkar*

National Centre for Biological Sciences, Tata Institute of Fundamental Research, UAS-GKVK Campus, Bangalore 560065, India

Many proteins display complex folding kinetics, which represent multiple parallel folding pathways emanating from multiple unfolded forms and converging to the unique native form. The small protein thioredoxin from *Escherichia coli* is one such protein. The effect of the chaperonin GroEL on modulating the complex energy landscape that separates the unfolded ensemble from the native state of thioredoxin has been studied. It is shown that while the fluorescence change accompanying folding occurs in five kinetic phases in the absence of GroEL, only the two slowest kinetic phases are discernible in the presence of saturating concentrations of GroEL. This result is shown to be consistent with only one out of several available folding routes being operational in the presence of GroEL. It is shown that native protein, which forms *via* fast as well as slow routes in the absence of GroEL, forms only *via* a slow route in its presence. The effect of GroEL on the folding of thioredoxin is shown to be the consequence of it binding differentially to the many folding-competent forms. While some of these forms can continue folding when bound to GroEL, others cannot. All molecules are then drawn into the operational folding route by the law of mass action. This observation indicates a new role for GroEL, which is to bias the energy landscape of a folding polypeptide towards fewer available pathways. It is suggested that such channeling might be a mechanism to avoid possible aggregation-prone routes available to a refolding polypeptide *in vivo*.

© 2001 Academic Press

Keywords: GroEL; thioredoxin; chaperone; energy landscape; folding pathway

*Corresponding author

Introduction

The ability of the *Escherichia coli* chaperonin GroEL to recognize and bind to hydrophobic surfaces of aggregation-prone polypeptides is crucial to its function.¹ Following capture of the substrate protein, binding of co-chaperonin GroES and ATP trigger a conformational change in GroEL, leading to a decrease in binding affinity.^{2,3} The folding polypeptide is then released into the cylindrical cavity of GroEL, which is capped by co-chaperonin GroES,⁴ and which provides a passive cage for folding in seclusion;⁵ hence, competing aggregation processes are avoided. The ATP-dependent reaction cycle of GroEL interacting with its co-chaperone GroES, and their effect on the refolding

polypeptide are understood relatively well.^{6–9} The kinetic and molecular events at the level of the refolding polypeptide are, however, still comparatively obscure. More recent studies have indicated that GroEL plays a more active role in optimizing folding,^{10–16} and it appears that this active role may primarily be the consequence of binding energy being exploited to effect changes in the conformation of the substrate protein. Thus, the binding energy of GroEL may be utilized to unfold partially folded or mis-folded proteins either by decreasing the activation energy for unfolding^{11,12} or by thermodynamic coupling.¹³ Conformational changes in GroEL that result from GroES and ATP binding may lead to mechanical unfolding of the substrate protein.¹⁴ Binding to GroEL can also result in the acceleration of folding of some substrate proteins: the binding energy may promote inter-domain reorganization¹⁵ as suggested for lysozyme, or effect a thermodynamic shift to increase the concentration of folding-competent forms as in the case of barstar.¹⁶

Abbreviations used: Trx, thioredoxin; ANS, 8-anilino-1-naphthalene sulfonic acid; GdnHCl, guanidine hydrochloride; CNBr, cyanogen bromide.

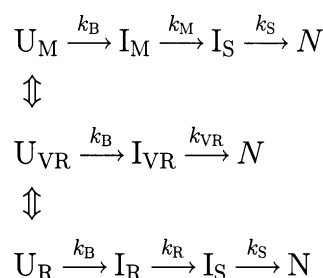
E-mail address of the corresponding author: jayant@ncbs.res.in

Thus, the active role of the chaperonins is envisaged mainly as minimizing or rescuing kinetically trapped intermediates *via* binding and consequent unfolding, thereby improving the yield of refolding. In this way, the energy landscape for folding can be modulated.^{17–19} It has been suggested that binding and hydrolysis of ATP can provide GroEL with the energy to alter and perhaps smooth the energy landscape available to the substrate protein for folding.^{20,21} Even without ATP hydrolysis, the energy landscape of the substrate can be modified, because binding of GroEL alters the kinetic barriers that separate various forms present at similar or lower-energy rungs in the folding funnel. In this manner, GroEL may be able to optimize folding by channeling the folding polypeptide along some preferred routes, when many routes are otherwise available. While modulation of the energy landscape in this way has been shown to be possible through mutations in the case of *E. coli* dihydrofolate reductase, which result in four folding channels collapsing into only two,²² such modulation through the action of a chaperonin has not been reported previously.

Here, we study the effect of GroEL on the complex refolding kinetics^{23–27} of oxidized thioredoxin (Trx) from *E. coli*. Trx is an oxidoreductase, whose sequence of 108 amino acid residues folds into a large $\beta\alpha\beta\alpha\beta$ domain and a small $\beta\beta\alpha$ domain.²⁸ Previous studies have shown that multiple parallel routes are utilized for folding to the native (N) state of Trx.²⁷ Thus, Trx is a good model substrate protein to study whether GroEL can differentially affect parallel folding routes by modulating the energy landscape accessible for folding.

Equilibrium unfolded Trx consists of at least three unfolded forms,^{23,27} presumably because of the presence of five proline residues that may be in *cis* or *trans* conformations; a very rapidly refolding form, U_{VR} , a rapidly refolding form, U_R , and a medium/slow refolding form, U_M . Native Trx unfolds rapidly to U_{VR} , which then relaxes slowly *via* two parallel, presumably proline isomerization-dependent processes, to U_R and U_M . The refolding kinetics of Trx have been investigated in detail using many probes, including tryptophan fluorescence, far-UV circular dichroism (CD), near-UV CD, 8-anilino-1-naphthalene sulfonic acid (ANS) binding, and regain of native Trx activity,^{23–27} and Scheme 1 shows the mechanism that has been proposed to describe the refolding of equilibrium unfolded Trx:

All three unfolded forms initially form burst-phase intermediates in parallel reactions. The early burst-phase intermediate ensemble consists of predominantly β structures, native as well as non-native, that have yet to stabilize.²⁷ Molecules in the burst-phase ensemble that originate as U_{VR} then fold directly to N, while molecules that originate as U_R and U_M fold to the slow-folding intermediate I_S , whose transformation to N is accompanied by *trans* to *cis* isomerization of Pro76, the only *cis* proline residue in the N state.²⁶ The folding of wild-



Scheme 1.

type Trx occurs in four observable kinetic phases and one unobservable burst-phase, and replacement of Pro76 by Ala eliminates only the slowest-folding phase.²⁶ Transitions between I_{VR} , I_R and I_M within the burst-phase intermediate ensemble are not ruled out in Scheme 1, and are expected to occur rapidly relative to the rates at which these burst-phase intermediates fold further.

Here, the effect of GroEL on the parallel folding pathways of Trx has been studied. In the presence of a saturating concentration of GroEL, only the two slowest phases of fluorescence-monitored folding are observed, out of the four observed in the absence of GroEL. It is shown that the refolding of Trx proceeds *via* only the slowest of the two kinetic routes that are available for the formation of N in the absence of GroEL. The molecules that fold *via* the fast route in the absence of GroEL appear to be channeled to N *via* the slow route when GroEL is present.

Results

Folding and unfolding of Trx in the absence of GroEL

To determine the effect of GroEL on the folding of Trx, it was first necessary to confirm that Scheme 1 indeed describes, correctly, folding in the absence of chaperone. The guanidine hydrochloride (GdnHCl)-induced equilibrium unfolding transition of Trx, monitored using fluorescence of the Trp residues at positions 28 and 31 as the tertiary structure probe, is shown in Figure 1(a). The Trp fluorescence is quenched strongly in N, because of the proximity of the active-site disulphide between Cys32 and Cys35.²⁹ There is a release of Trp quenching upon unfolding, with the mid-point of the equilibrium unfolding transition being at 2.5 M GdnHCl. The increase in fluorescence upon unfolding occurs in one kinetic phase, as seen in Figure 1(b) for unfolding in 3.2 M GdnHCl or in 4.8 M GdnHCl (inset), and corresponds to the formation of U_{VR} . The unfolding rates show a steep dependence on GdnHCl concentrations,²⁴ with a rate of 0.02 s⁻¹ in 3.2 M GdnHCl and 3 s⁻¹ in 4.8 M GdnHCl. Figure 1(c) shows that when Trx, which had been unfolded to equilibrium in 3.6 M

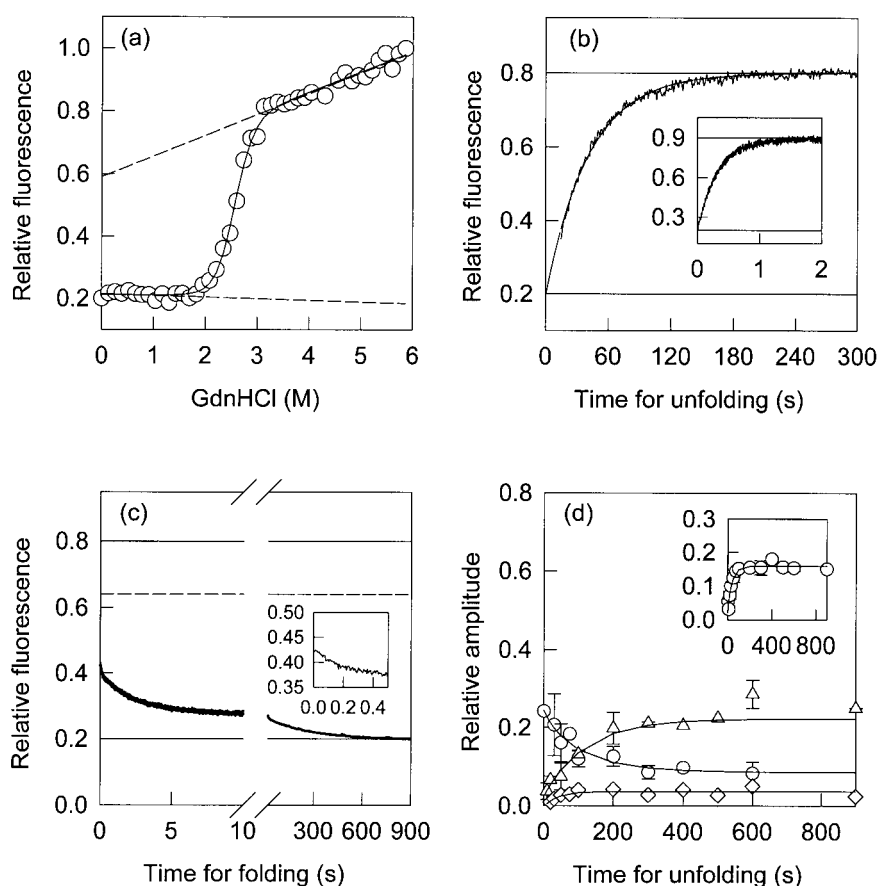


Figure 1. Folding of Trx in the absence of GroEL. (a) Equilibrium unfolding of thioredoxin. The relative intrinsic Trp fluorescence of Trx equilibrated in different concentrations of GdnHCl is plotted against GdnHCl concentration. The broken lines represent the extrapolated unfolded and the native baselines. The continuous line through the data is a fit of the data to a two-state $N \rightleftharpoons U$ model⁴⁵ and yields a C_M value of 2.55 M. (b) Kinetics of unfolding of thioredoxin in 3.2 M GdnHCl, and 4.8 M GdnHCl (inset). The upper continuous lines represent the fluorescence of the unfolded protein in 3.2 M and 4.8 M GdnHCl (inset), and the lower continuous lines represent the fluorescence of N. (c) Kinetics of folding of equilibrium-unfolded Trx in 0.3 M GdnHCl. The progress of the folding reaction was monitored by measurement of the intrinsic Trp fluorescence of Trx. The upper continuous line represents the fluorescence of unfolded protein in 3.6 M GdnHCl, the lower continuous line represents the fluorescence of N, and the broken line represents the value of the fluorescence of unfolded protein in 0.3 M GdnHCl, obtained by linear extrapolation of the unfolded protein baseline in (a). The inset shows the fluorescence change occurring in the first 0.5 second after commencement of refolding. (d) Kinetics of refolding of transiently unfolded Trx. Trx was unfolded in 4.8 M GdnHCl for each of the different times indicated before being refolded by dilution to 0.3 M GdnHCl. The relative amplitudes of the very rapid (○), rapid (△) and medium phases (◇) of fluorescence change are plotted against the time at which refolding is commenced. The relative amplitudes of the slow phase are shown in the inset. The error bars represent the standard deviations from three separate experiments.

GdnHCl, is refolded in 0.3 M GdnHCl, the folding to the native state occurs *via* a burst-phase and four observable phases of decreasing Trp fluorescence. The burst-phase change in fluorescence as well as the subsequent very rapid phase of fluorescence change that has an apparent rate constant of 5 s^{-1} , are shown in the inset to Figure 1(c). The rapid, medium and slow phases that follow have apparent rate constants of 0.3, 0.02 and 0.004 s^{-1} , respectively. These observable phases have been attributed to the $I_{VR} \rightarrow N$ (very rapid phase), $I_R \rightarrow I_S$ (rapid phase), $I_M \rightarrow I_S$ (medium phase) and $I_S \rightarrow N$ (slow phase) steps of Scheme 1.²⁷

To confirm the presence of three unfolded forms, native Trx was transiently unfolded in 4.8 M GdnHCl, for times ranging from 1 to 900 seconds,

and then refolded in 0.3 M GdnHCl. At one second of unfolding, native Trx is expected to unfold completely to U_{VR} (Figure 1(b)) and, as expected, the folding kinetics show only a burst-phase followed by a very rapid phase of fluorescence change. As shown in Figure 1(d), with increasing time of unfolding, the relative refolding amplitude of the very rapid folding phase decreases, while that of the rapid and medium phases build up. The decrease in the very rapid phase amplitude occurs in two phases, with relaxation rates of 0.025 and 0.008 s^{-1} . The relative amplitudes of the rapid and medium phases build up with rates of 0.008 and 0.025 s^{-1} , respectively. Thus, in the unfolded ensemble, U_{VR} equilibrates with U_R and U_M with relaxation rates of 0.008 and 0.025 s^{-1} , respectively.

The relative amplitude of the slow phase, i.e. the $I_S \rightarrow N$ transition, builds up with a rate of 0.025 s^{-1} as shown in the inset to Figure 1(d). These observations confirm that, as suggested in earlier studies, there exist three different unfolded forms of Trx that arise in the denatured ensemble, presumably due to proline isomerizations.

Previously, the existence of two channels leading to N, with 10% of the molecules forming N very rapidly from U_{VR} , and 90% of the molecules forming N slowly from I_S , had been confirmed by experiments showing that 10% of refolding molecules regained Trx activity very rapidly, while 90% of the molecules regained activity with the same rate as that of the slow phase of fluorescence change.²⁷ Here, the existence of the fast and slow channels leading to N is confirmed by a double-jump ($U \rightarrow N \rightarrow U$) assay in which equilibrium-unfolded Trx was refolded for variable time intervals, and then re-unfolded to assess the amount of N present at the time refolding was interrupted. Figure 2(a) shows the kinetics of unfolding in 3.2 M GdnHCl, when unfolding is initiated after folding in 0.3 M GdnHCl has proceeded for ten seconds and for 100 seconds. While the apparent rates of the kinetic unfolding traces are the same and equal to the rate at which N unfolds in 3.2 M GdnHCl (Figure 1(b)), the amplitudes increase with an increase in the time at which folding is interrupted. The relative amplitudes represent the amount of N present at the time refolding was interrupted. For example, it is seen that 10% of the refolding molecules have formed N at ten seconds of refolding itself, because the amplitude of the kinetic trace of unfolding, when refolding is interrupted at ten seconds, is 10% of the amplitude observed of the kinetic trace of unfolding of an identical concentration of fully native Trx. Figure 2(b) shows how the fraction of the native molecules, as determined from such double-jump assays, increases with time of refolding. It is observed that, while 10% of the molecules have formed N at ten seconds of refolding, i.e. *via* the fast channel, the remaining 90% form N in a single phase that corresponds in rate to that of the slow phase of fluorescence change (0.004 s^{-1}) i.e. *via* the slow channel. Thus, the data in Figures 1 and 2 confirm the basic features of Trx refolding described earlier²⁷ and by Scheme 1.

Folding of Trx in the presence of GroEL

Since GroEL is devoid of Trp residues, the intrinsic Trp fluorescence of Trx can be used as the probe to study the effect of GroEL on Trx refolding. Figure 3 shows that the relative amplitudes of the burst, very rapid and rapid phases of change in fluorescence decrease with increasing concentration of GroEL. The decreases in the relative amplitudes of the three fastest phases is compensated for by increases in the amplitudes of the medium and slow phases (Figure 3(a)). The relative amplitude of the burst-phase decreases from 45% in the

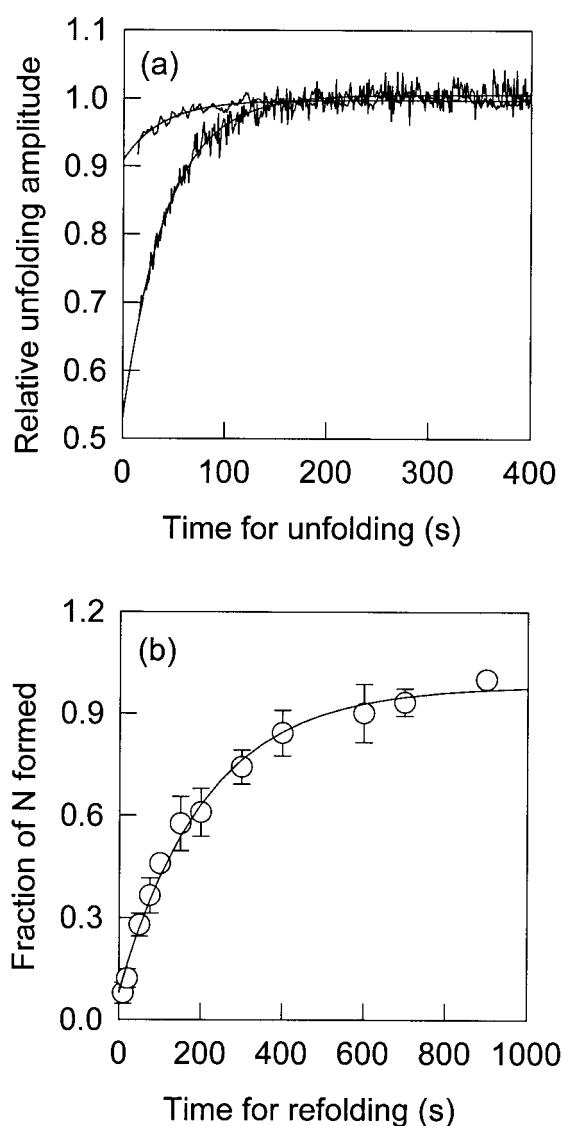


Figure 2. Fractional formation of N upon transient refolding. Thioredoxin that had been unfolded to equilibrium in 3.6 M GdnHCl was refolded by dilution to 0.3 M GdnHCl for the indicated time intervals, and then unfolded in 3.2 M GdnHCl. (a) Unfolding kinetics of equilibrium-unfolded Trx that has been refolded for ten seconds (upper trace) and 100 seconds (lower trace). Unfolding was monitored by Trp fluorescence at 368 nm, and the data were normalized to a value of 1 corresponding to the value of fluorescence when the unfolding reaction is complete. (b) The relative amplitudes of the unfolding reaction, obtained after refolding for different times, were normalized by taking the unfolding amplitude of equimolar native protein as 1, thereby defining the fraction of N formed at different times. The continuous line through the data represents a non-linear, least-squares fit of the data to a single exponential.

absence of GroEL to become zero at a saturating concentration of GroEL (Figure 3(b)), at which the ratio of concentration of GroEL to that of Trx is approximately 1:1.

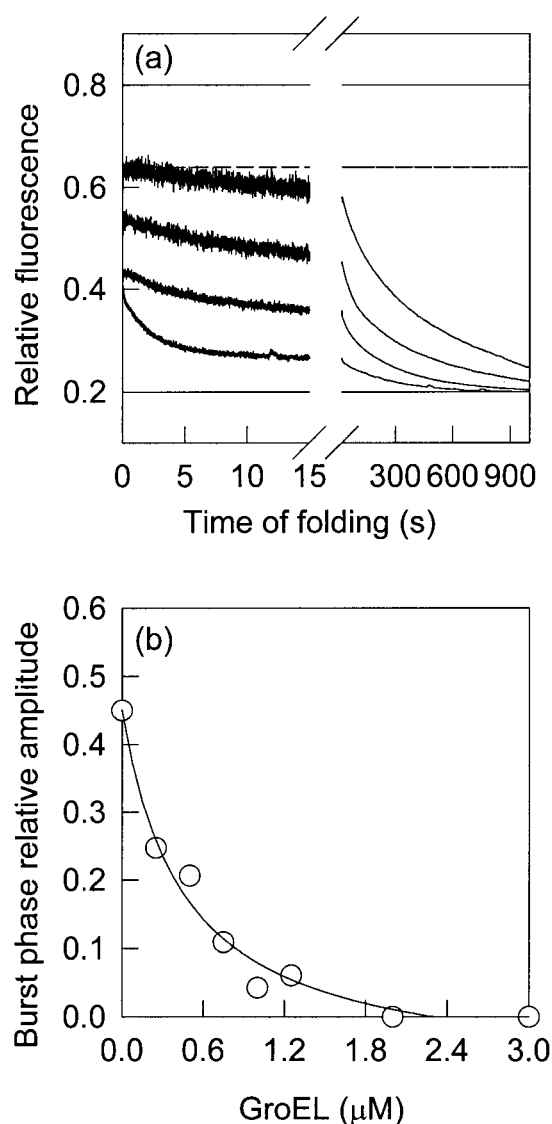


Figure 3. Kinetics of folding of Trx in the presence of GroEL. (a) Refolding of thioredoxin in the absence and presence of different concentrations of GroEL. Trx (1.5 μM) was refolded in 0.3 M GdnHCl in the absence (lowest trace) and in the presence of 0.5, 1 and 1.5 μM GroEL (upper traces). The upper and lower continuous lines represent the fluorescence values of unfolded protein in 3.6 M GdnHCl, and of native protein, respectively, and the broken line represents the value of the fluorescence of unfolded protein in 0.3 M GdnHCl, obtained by linear extrapolation of the unfolded protein baseline in Figure 1(a). (b) Relative amplitude of the unobserved burst-phase as a function of GroEL concentration. The relative burst-phase was determined as the unobservable amplitude divided by the total amplitude of the folding reaction. The continuous line through the data has been drawn by inspection only.

To determine whether the effect of GroEL on the two slowest phases of folding is due to specific binding of Trx inside the GroEL cavity, the exper-

iment shown in Figure 3(a) was repeated with GroEL that had been pre-saturated with rhodanese, a stringent substrate of GroEL, known to bind inside the GroEL cavity.^{15,16} The rates and amplitudes of the two slowest phases of folding in the presence of rhodanese-saturated GroEL are identical with those observed in the absence of GroEL (data not shown), indicating that the effect seen with GroEL alone is indeed due to specific binding of Trx inside the GroEL cavity, and is not due to non-specific binding.

Figure 3(a) shows that native Trx does not bind GroEL: the same final fluorescence of N is recovered in the presence or absence of GroEL. Activity measurements of Trx folded in the presence of GroEL also confirm that all the molecules fold to free N in the presence of GroEL: the activity is identical with that of an equimolar concentration of free Trx; moreover, the activity is unaffected by prolonged incubation with GroEL (data not shown). GroEL can, however, bind unfolded Trx molecules, as shown by its ability to bind two CNBr-generated fragments of thioredoxin,³⁰ which are unstructured at neutral pH (unpublished results).

Figure 4 shows the effect of GroEL on the relative amplitudes and apparent rates of all the observable phases. The very rapid phase disappears at sub-stoichiometric concentrations of GroEL, while the rapid phase disappears only at equimolar concentrations of GroEL. The medium and slow phases show a fourfold and a 5.3-fold increase in relative amplitude, respectively. The apparent rates of the rapid and slow folding phases decrease significantly with increasing GroEL concentration, while the rate of the medium phase decreases marginally. At saturating concentrations of GroEL, the rates of the medium and slow phases level off at a non-zero value, while the rate of the rapid phase becomes zero. The dependences of the rates of the observed rapid, medium and slow phases on GroEL concentration were analyzed according to equation (1)³¹ to yield values for the dissociation constant, K_D , of 0.2, 0.07 and 0.2 μM for GroEL binding to I_R , I_M and I_S , respectively. The value of the dissociation constant for I_M is only a crude estimate due to the scatter in the data. Similar values for the dissociation constants are obtained from fitting the dependence of the relative amplitudes of the rapid, medium and slow phases on GroEL concentrations according to a simple binding curve (equation (2)).

Effect of delayed addition of GroEL on Trx refolding

In a delayed addition experiment, equimolar GroEL was added at different time intervals after commencement of folding in 0.3 M GdnHCl (Figure 5(a)). At each time of addition of GroEL, there is an increase in the fluorescence that accompanies its binding to the intermediate forms pre-

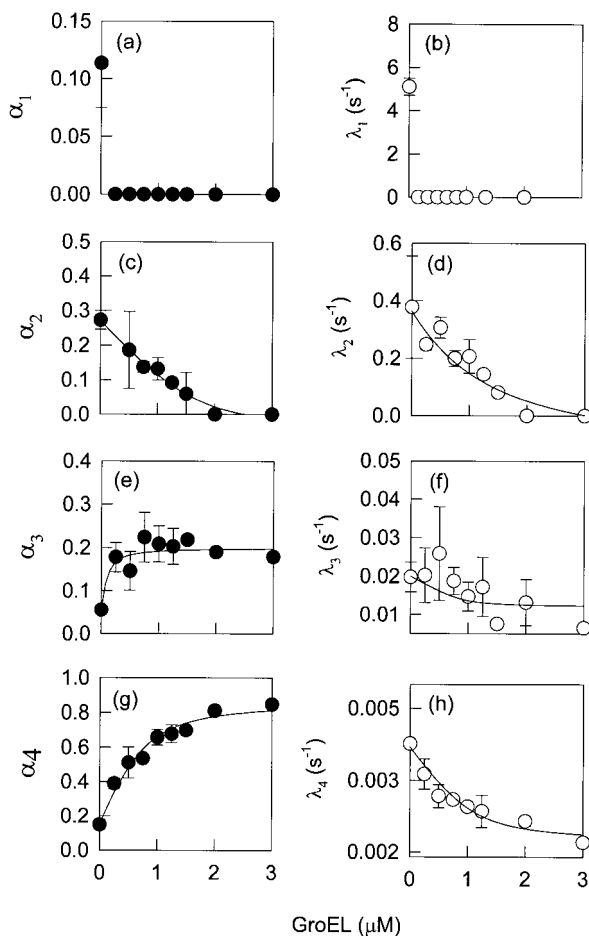


Figure 4. Effect of GroEL on the folding kinetics of Trx. (a) and (b) Relative amplitude and observed rate constant of the very rapid phase; (c) and (d), relative amplitude and observed rate constant of the rapid phase; (e) and (f), relative amplitude and observed rate constant of the medium phase; (g) and (h), relative amplitude and observed rate constant of the slow phase. The error bars represent standard deviations from at least three different experiments. The continuous lines through the data in (c), (e) and (g) represent fits to equation (2), and those through the data in (d), (f) and (h) represent fits to equation (1),³¹ and yield estimates of the dissociation constants for GroEL binding to various intermediates as described in the text.

sent, which is complete in the ten seconds dead-time of mixing. This increase in fluorescence is to the fluorescence value (within 10%) seen for molecules that have folded for the same time when folding is commenced in the presence of GroEL. With increasing times of folding before addition of GroEL, smaller and smaller increases in fluorescence are seen, because molecules are transformed to N, which does not bind GroEL. The decrease in the value of the initial fluorescence of the GroEL-bound molecules follows the kinetic trace of fluorescence change obtained when folding is initiated in the presence of GroEL.

Effect of GroEL on the folding of transiently unfolded Trx

Figure 5(b) compares the folding kinetics of transiently unfolded Trx in the presence and absence of GroEL. Trx was unfolded in 4.8 M GdnHCl for ten seconds, before being refolded in 0.3 M GdnHCl in the presence or absence of GroEL. In the presence of equimolar GroEL, the relative amplitude of the burst-phase seen for the folding of transiently unfolded protein is reduced from 45 to 30%, while for equilibrium unfolded protein it is reduced to essentially zero (Figure 3). As in the case of the refolding of equilibrium unfolded Trx in the presence of equimolar GroEL, the only observable refolding phases for transiently unfolded Trx in the presence of equimolar GroEL are the medium and slow phases: the very rapid and rapid phases are absent.

Double-jump assay for formation of N in the presence of GroEL

It was possible to carry out the double-jump assay for N (Figure 2) in the presence of GroEL also, because N does not bind GroEL (see above). This is evident from the observations that N unfolds at the same rate in the presence or absence of GroEL, and the fluorescence change that accompanies unfolding of 100% N molecules does not depend on whether GroEL is present (data not shown). Figure 6(a) shows that no unfolding reaction corresponding in rate to the unfolding of N is observed when unfolding is initiated after 30 seconds of folding; indicating that no N molecules are present even at 30 seconds after folding is commenced in the presence of GroEL. In contrast, 10% of the molecules form N at ten seconds of folding in the absence of GroEL (Figure 2). Hence, it appears that the fast channel for folding to N is no longer operational in the presence of GroEL. This result is emphasized in Figure 6(b), where the kinetics of formation of N in the presence of GroEL are shown. The apparent rate of formation of N in the presence of GroEL is 0.003 s^{-1} , which is similar to the slow rate of change in fluorescence measured in the presence of GroEL (Figure 4). Extrapolation of the kinetic curve for formation of N to $t=0$ clearly shows that no N is formed in the first 30 seconds of folding. A lag is seen in the formation of N when folding of Trx occurs in the presence of an equimolar concentration of GroEL (Figure 6(b) and inset). Indeed, such a lag would be expected if N forms from I_M in a two-step process. The kinetics of formation of N fit well to equation (3), which describes the formation of N in two consecutive steps³² with rates of 0.02 s^{-1} and 0.003 s^{-1} .

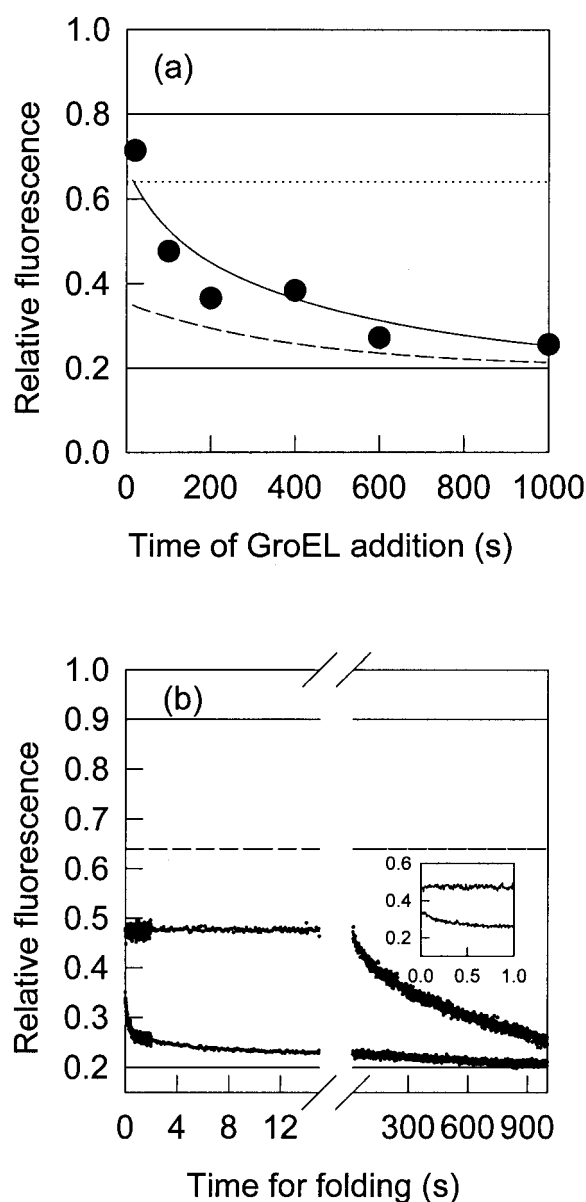


Figure 5. (a) Effect of delayed addition of GroEL on the folding kinetics of Trx. Trx that had been unfolded to equilibrium in 3.6 M GdnHCl was refolded in 0.3 M GdnHCl for varying periods of time before addition of GroEL to a final concentration of 1.5 μ M (same as the final concentration of Trx). The upper and lower continuous lines represent the fluorescence values of unfolded protein in 3.6 M GdnHCl, and of native protein, respectively, and the dotted line represents the value of the fluorescence of unfolded protein in 0.3 M GdnHCl, obtained by linear extrapolation of the unfolded protein baseline in Figure 1(a). The broken trace shows the change in fluorescence during folding when no GroEL is present. The continuous trace shows the change in fluorescence when folding is initiated in the presence of 1.5 μ M GroEL. Both the traces were obtained from manual-mixing experiments with a dead-time of ten seconds. The filled circle at each time-point represents the fluorescence when 1.5 μ M GroEL has been added to the folding protein solution, at that time. The subsequent decrease in fluorescence, as Trx folds further, follows the continuous trace from the time of addition. (b) Effect of GroEL on the kinetics of refolding

Discussion

Altered folding kinetics in the presence of GroEL

Two observations suggest that the basic folding mechanism of Trx is not altered in the presence of GroEL. (1) For the rapid, medium or slow phase, the dependences on GroEL concentration of the rate and amplitude fit well to simple binding curves described by equations (1) and (2), respectively (Figure 4). Extrapolations of the binding curves to zero GroEL concentration correctly predict the rate and amplitude observed for each phase in the absence of GroEL. (2) The same kinetic trace of fluorescence change is recovered, whether GroEL is added at the commencement of refolding or after different delays after the commencement of refolding (Figure 5(a)). These observations suggest that the different intermediate forms that populate the folding pathways of Trx are also there in the presence of GroEL, and that the changes in amplitudes and rates that are observed in the presence of GroEL are the consequence of GroEL binding to these intermediate forms.

Binding of GroEL increases the intrinsic Trp fluorescence of folding Trx molecules

The 5.3-fold increase in the relative amplitude of the slow phase, i.e. $I_S \rightarrow N$, at saturating GroEL concentrations is surprising, because 90% of the molecules fold to N with this rate in the absence of GroEL (Figure 2(b)) and, even if the remaining 10% molecules fold to N *via* the slow phase in the presence of GroEL, this would lead to only a 10% increase in the fluorescence change that accompanies the slow phase. It appears, therefore, that when GroEL is added either at the commencement of refolding or at any time later (Figure 5(a)), its binding to early forms on the refolding pathway of Trx leads to a very rapid increase in Trx fluorescence, presumably because the binding occurs very near the active site of Trx, where the two Trp residues are located. In the case of lysozyme¹⁵ and barnase³³ too, binding of GroEL is accompanied by an increase in the intrinsic Trp fluorescence of the substrate protein.

of transiently unfolded Trx. Native Trx was unfolded in 4.8 M GdnHCl for ten seconds before being refolded by dilution to 0.3 M GdnHCl in the absence of any GroEL (lower trace) and in the presence of 3 μ M (equimolar) GroEL (upper trace). The upper continuous line represents the fluorescence of unfolded protein in 4.8 M GdnHCl, the lower continuous line represents the fluorescence of native protein, and the broken line represents the value of the fluorescence of unfolded protein in 0.3 M GdnHCl, obtained by linear extrapolation of the unfolded protein baseline in Figure 1(a). The inset shows the fluorescence changes that occur during the first one second of refolding.

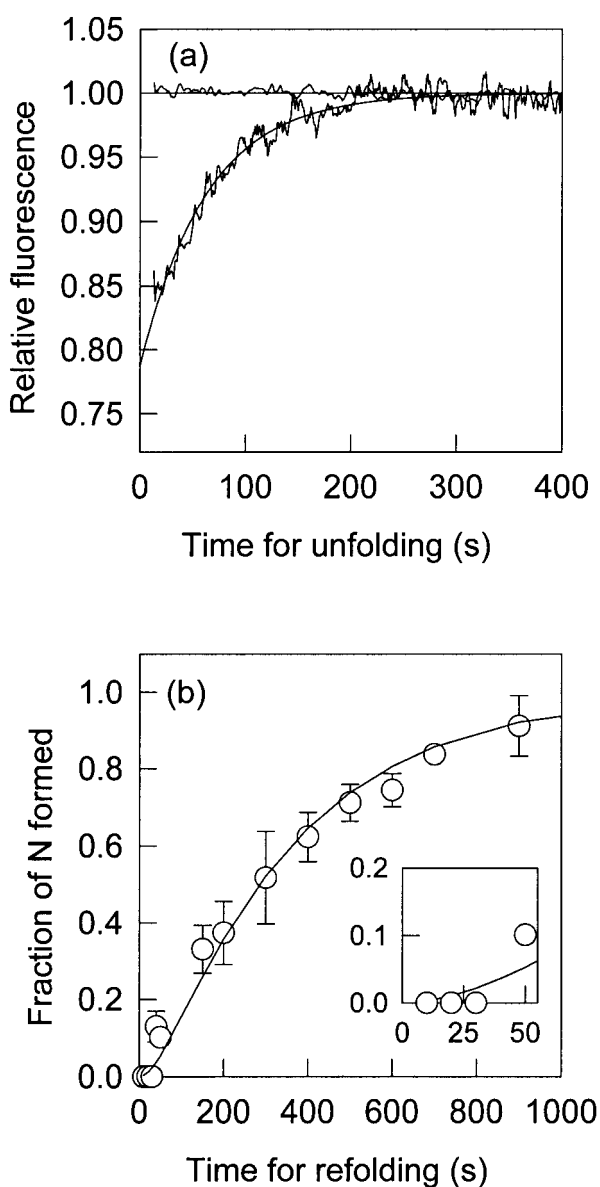


Figure 6. Kinetics of unfolding of transiently folded Trx. (a) Equilibrium unfolded Trx in 3.6 M GdnHCl was refolded in 0.3 M GdnHCl for 30 seconds (upper trace) and 75 seconds (lower trace) in the presence of 3 μ M GroEL (equimolar) before being unfolded in 3.2 M GdnHCl. Unfolding was monitored by Trp fluorescence at 368 nm, and the data were normalized to a value of 1 corresponding to the value of fluorescence when the unfolding reaction is complete. (b) Effect of GroEL on the kinetics of formation of N. A double jump-assay, as described for Figure 2, was used to determine the fractional formation of native protein at different times after commencement of folding. Trx that had been unfolded to equilibrium in 3.6 M GdnHCl was refolded by dilution to 0.3 M GdnHCl in the presence of 3.3 μ M GroEL (equimolar) before being unfolded in 3.2 M GdnHCl. The continuous line through the data obtained in the presence of equimolar GroEL represents a fit to equation (3).³² The inset shows the fraction of native protein formed at early times of refolding.

For the refolding of equilibrium-unfolded Trx, the absence of the burst-phase change in fluorescence at saturating GroEL concentrations could be either because the burst-phase intermediate ensemble does not form or because the increase in Trx fluorescence that occurs when the unfolded and burst-phase intermediate ensembles bind to GroEL, exactly compensates for the decrease in fluorescence that would otherwise be observed when the unfolded ensemble transforms to the burst-phase ensemble. The different members of the burst-phase ensemble, I_{VR} , I_R and I_M , are expected to differ in their fluorescence properties. Thus, if the folding of U_{VR} alone is initiated in the presence of a saturating concentration of GroEL, then it is possible that the burst-phase decrease in fluorescence that occurs during the $U_{VR} \rightarrow I_{VR}$ transition is not fully compensated for by the increase that occurs upon GroEL binding to U_{VR} and possibly I_{VR} as well. Figure 5(b) shows that this is indeed so: when Trx is transiently unfolded for only ten seconds so that U_{VR} is predominantly present, and then refolded in the presence of saturating GroEL, a burst-phase change in fluorescence is still observed. Thus, I_{VR} bound to GroEL does form in the presence of saturating GroEL, but its fluorescence is lower than that of U_{VR} . Figure 5(b) therefore rules out the possibility that the burst-phase ensemble itself does not form from equilibrium unfolded Trx in the presence of saturating GroEL (Figure 3(b)). The absence of a burst-phase change in fluorescence for folding in the presence of 1.5 μ M GroEL (equimolar to Trx), suggests that the binding of GroEL occurs during the 6 ms instrumental dead-time; consequently, the bimolecular rate constant for association must be $>5 \times 10^8 \text{ M}^{-1} \text{ s}^{-1}$. Indeed, GroEL is known to be capable of binding its substrate proteins at diffusion-controlled rates.^{18,34}

Binding of GroEL to intermediate forms reduces the rates of folding

When bound by GroEL, folding intermediates may or may not be capable of further folding. In the former case, as seen for hen lysozyme,¹⁵ barstar,¹⁶ barnase,³³ chymotrypsin inhibitor-2,³¹ staphylococcal nuclease,³⁵ α -lactalbumin,³⁶ and maltose-binding protein,³⁷ folding rates have non-zero values at saturating concentrations of GroEL.^{31,33} In the latter case, exemplified by rhodanese,³⁸ α -lactalbumin³⁶ and human dihydrofolate reductase,³⁹ the folding rate will be zero at saturating GroEL concentrations, because virtually all protein molecules will be GroEL-bound. Moreover, the decrease in folding rates with increasing GroEL concentration will match the decrease in amplitude, because the fraction of the folding-competent GroEL-free form³¹ decreases with increasing GroEL concentration (equations (1) and (2)).

Thus, the data in Figure 4 suggest that I_R and I_{VR} cannot fold further when bound by GroEL, because the very rapid and rapid rates decrease to

zero at saturating GroEL concentrations, while I_M and I_S , as well as the corresponding unfolded forms can, because the medium and slow rates decrease to non-zero values independent of GroEL concentration. Upon binding of GroEL, the stabilization of I_M and I_S increases the effective energy barriers between them and the next sequential forms on the refolding pathway, but only so much as to slow folding, while the stabilization of I_{VR} and I_R is large enough to effectively stop their further folding.

The decrease seen for the very rapid rate occurs at a tenfold lower concentration of GroEL than that seen for the rapid rate, indicating that I_{VR} binds GroEL at least tenfold more tightly than I_R . The GroEL concentration-independent folding rates of I_M and I_S at saturating GroEL concentrations correspond to the folding rates of GroEL-bound forms, because virtually all protein molecules are expected to be bound by GroEL. The binding of GroEL to U_M , U_S , I_M and I_S appears to be much faster than their subsequent folding, because the medium and slow-phase rates still fit to single exponentials at lower concentrations of GroEL, where both GroEL-bound and free forms of I_M and I_S are present. If this were not the case, rates corresponding to the folding of the GroEL-bound as well as the free forms would have been observed.³¹ Using the values obtained for the dissociation constant, K_D , for GroEL binding to the I_R , I_M and I_S forms, of 0.2, 0.07 and 0.2 μM , respectively (see Results) (which are within the micro- to nanomolar range of dissociation constants for GroEL binding to the intermediate forms of other proteins¹⁸), and a value of $5 \times 10^8 \text{ M}^{-1}\text{s}^{-1}$ for the bimolecular rate constant for GroEL binding (see above), the estimated dissociation rates of GroEL from I_R , I_M and I_S are 100, 35 and 100 s^{-1} , respectively. Thus, the rates of GroEL binding to and dissociating from either I_R , I_M or I_S are indeed faster than the rates of further folding of these forms in the presence of GroEL.

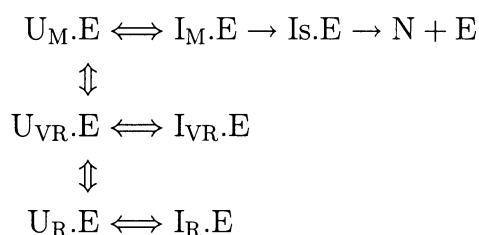
Formation of N in the presence of GroEL

When GroEL is absent, 10% of the molecules form N in a sub-second phase, and no lag is seen in the formation of N (Figure 2). In the presence of an equimolar concentration of GroEL, a distinct lag in the formation of N is observed, after which all molecules form N in a single-exponential process with a time-constant of 0.003 s^{-1} , which corresponds to the rate of the slow phase of fluorescence change that accompanies folding in the presence of GroEL. The magnitude of the lag time suggests that the last step in the formation of N, which has a rate of 0.003 s^{-1} , is preceded by a faster step with a rate of 0.02 s^{-1} (Figure 6). The rate of the faster step corresponds to the rate of the medium phase of fluorescence change in the presence of GroEL (Figure 4). These observations imply that (1) the fast channel for formation of N is no longer operative in the presence of GroEL, and (2) the lag in the formation of N in the presence of

GroEL is because of the time taken for the concentration of GroEL-bound I_S to build up as GroEL-bound I_M folds further to N. These conclusions are supported by the observations that (1) the very rapid phase of fluorescence change, which is known to accompany the $I_{VR} \rightarrow \text{N}$ reaction that constitutes the fast channel for formation of N in the absence of GroEL (Figure 3), is absent in the presence of an equimolar concentration of GroEL (Figure 6), and (2) the rapid phase of fluorescence change, which is known to accompany the $I_R \rightarrow 6I_S$ reaction in the absence of GroEL, is absent in the presence of an equimolar concentration of GroEL (Figure 4). It should be noted that because there are two routes to the formation of I_S in the absence of GroEL (Scheme 1), there is no lag seen in the formation of N in those conditions: the rate of the $I_R \rightarrow I_S$ reaction is such that it contributes to the buildup of N in a time-frame that would otherwise correspond to the lag period in which the population of I_S builds up from I_M .

Mechanism of refolding in the presence of GroEL

The disappearance of the very rapid and rapid phases, as well as the disappearance of the fast channel for the formation of N, at saturating concentrations of GroEL, suggest that I_{VR} and I_R are incapable of folding to N and I_S , respectively, after being bound by GroEL. As discussed above, I_M and I_S fold in GroEL-bound forms in the presence of saturating GroEL. Since all Trx molecules finally fold to free N in the presence of GroEL (see above), GroEL-bound I_{VR} and I_R , as well as GroEL-bound U_{VR} and U_R , must fold to N only by transiting through the GroEL-bound U_M form. Thus, in the presence of saturating concentrations of GroEL, the folding of Trx is represented by Scheme 2, where X.E represents GroEL-bound forms:



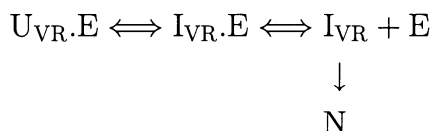
Scheme 2.

According to Scheme 2, all GroEL-bound refolding Trx molecules are channeled to N *via* one slow route. This channeling occurs because $U_{VR}.E$ and $U_R.E$ molecules would replenish $U_M.E$ molecules as they fold to N, because of thermodynamic coupling. Conceivably, $I_{VR}.E$ and $I_R.E$ molecules can similarly replenish $I_M.E$ molecules within the burst-phase intermediate ensemble itself; although this possibility is not shown explicitly in Scheme 2. It

should be noted that, although X is present predominantly in the form X.E in saturating concentrations of GroEL, X.E coexists with small amounts of free X and E, which are not shown in Scheme 2 so as not to complicate it unnecessarily.

Scheme 2 predicts that all Trx molecules should form N in the slow phase corresponding to the rate of the $I_S.E \rightarrow N + E$ reaction, and that no N molecule should form in a faster reaction as seen in the absence of GroEL (Figure 2), because the $I_{VR}.E \rightarrow N + E$ reaction cannot occur. The Scheme predicts the lag seen in the formation of N, because N forms from $I_M.E$ in a two-step process: $I_M.E \rightarrow I_S.E \rightarrow N + E$. Since the rates of the $I_M.E \rightarrow I_S.E$ and $I_S.E \rightarrow N + E$ reactions are 0.02 s^{-1} and 0.003 s^{-1} , respectively, in the presence of equimolar GroEL, and because the rates of all preceding steps leading to the formation of I_M appear to be faster than or similar to the rate of the $I_M.E \rightarrow I_S.E$ reaction, the lag of 30 seconds is expected.

An alternative explanation for the observation that N forms only in a single slow phase in the presence of GroEL, could be that the rate-limiting steps for folding are the release reactions from GroEL. In such a scenario, the observed folding rates for the different unfolded populations may appear to be similar, even when the actual folding rates are not different from the rates seen in the absence of GroEL. For example, the following alternative reaction scheme can be considered, for the fast-folding U_{VR} form:

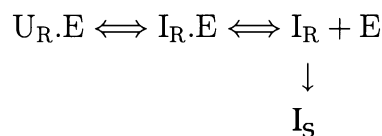


Scheme 3.

According to Scheme 2, the $I_{VR}.E \rightarrow N + E$ reaction does not operate at saturating GroEL concentration (see above). It is possible, however, that while N does not form directly from $I_{VR}.E$, it may form indirectly when GroEL transiently dissociates, and the free I_{VR} folds to N. Depending on the rate of dissociation of GroEL from $I_{VR}.E$, and on the K_D of GroEL binding to I_{VR} (the bimolecular association rate constant is $>5 \times 10^8 \text{ M}^{-1}\text{s}^{-1}$ (see above)), it is possible that the effective rate of formation of N from $I_{VR}.E$ is the same as the rate of formation of N from $I_S.E$. In such a scenario, there would be no channeling of molecules from the I_{VR} route to the I_S route. However, this possibility is easily ruled out, because the lag that is seen in the formation of N, is not predicted by Scheme 3. These results suggest that the K_D for GroEL binding to I_{VR} is less than 1 nM, because then the effective rate of formation of N according to Scheme 3 would be too slow to be significant. The K_D for GroEL binding to I_{VR} could not, however, be deter-

mined, as it has been for I_R , I_M and I_S , because it is too small to be measured. (Figure 4a).

It is difficult to distinguish clearly whether, in the presence of saturating GroEL concentrations, the build up of I_S occurs only *via* the $I_M.E \rightarrow I_S.E$ route (Scheme 2), or also *via* the folding of transiently released I_R directly to I_S . Scheme 4 can be considered for I_R , where the $I_R.E \rightarrow I_S + E$ reaction does not occur, as in Scheme 2, but I_S can form *via* transiently released I_R :



Scheme 4.

Given that the estimated bimolecular rate constant of association of GroEL for I_R is $>5 \times 10^8 \text{ M}^{-1}\text{s}^{-1}$ and the dissociation rate is 100 s^{-1} , it can be shown by kinetic simulation that it is possible for the effective rate of formation of I_S *via* Scheme 4 to be the same as the rate (0.02 s^{-1}) of the $I_M.E \rightarrow I_S.E$ reaction in Scheme 2. Hence, it is not possible to rule out that the build-up of I_S may occur also according to Scheme 4, and not only according to Scheme 2.

Relevance of channeling

The channeling role of GroEL that has been proposed here for Trx, whereby folding molecules are induced to follow one route to the native protein, may be relevant for staphylococcal nuclease, which, like Trx, has multiple unfolded forms and folds through multiple parallel pathways.^{40,41} For staphylococcal nuclease too, the relative amplitude of the slowest of the four observable phases of folding increases at the expense of the fastest phase, when folding is initiated in the presence of increasing concentrations of GroEL.³⁵

It seems almost paradoxical that for Trx, and perhaps also for staphylococcal nuclease,³⁵ it is the fast-folding route that stops operating in the presence of GroEL. As suggested here for Trx, this is because the faster-folding forms bind GroEL tighter than the slower-folding forms. GroEL recognizes and binds to exposed hydrophobic surfaces on its substrate proteins,^{1,5,18} and tighter binding implies that the bound surface is more hydrophobic. The presence of more exposed hydrophobic surface in unfolded forms or very early intermediate forms might be expected to allow these forms to fold faster if hydrophobic interactions play an important part in driving the folding process. Partly folded forms with binding surfaces that are very hydrophobic are also expected to aggregate in the crowded situation prevalent in the cell, and this intermolecular aggregation is prevented by tight binding to chaperone

proteins. The cost of tight binding to chaperones is that the bound substrate protein folds slower than the free protein, as is seen commonly^{33–37} and predicted theoretically.²¹ Nevertheless, by folding while bound to the chaperone, the protein avoids intermolecular aggregation.

It is noteworthy that the channeling of Trx folding along one kinetic route, which is effected by the binding of GroEL and subsequent thermodynamic coupling, has the unusual result that the 10% of the unfolded molecules that contain the Pro76 bond in the native-like *cis* conformation in the unfolded form (as U_{VR}) are first converted to an unfolded form (U_M) with the Pro76 bond in a non-native *trans* conformation, before folding to the N state. Even when all molecules start off as U_{VR} in transiently unfolded Trx, the very rapid and rapid kinetic phases are eliminated in saturating concentrations of GroEL, and all U_{VR} molecules fold *via* the slow channel (Figure 5(b)). The measured rate of 0.025 s^{-1} for the $U_{VR} \rightleftharpoons U_M$ equilibrium (Figure 1(d)) is consistent with the channeling process described by Scheme 2. It would appear that the possible benefit of channeled folding, of minimizing aggregation as described above, overrides the energetic costs of *cis* to *trans* proline isomerization.

The results presented here suggest that the binding of unfolded forms or early intermediates by GroEL can have a profound effect on the energy landscape available to the protein molecules for folding. Binding of GroEL to some partly folded forms may prevent their folding further along a particular route, and folding protein molecules are channeled along alternative routes. The effect of this function is that the chaperone may provide biological assistance to a nascent polypeptide for exploring only a few pathways to the native state.

Materials and Methods

Protein purification

E. coli BL21(DE 3) cells containing the plasmid pET-trx⁴² were grown in rich medium containing 100 µg/ml of ampicillin at 37°C for 15 hours, and then harvested by centrifugation. The cell pellet was dissolved in residual medium, and Trx was extracted by osmotic shock by adding chloroform⁴³ and incubating the solution at 25°C for 15 minutes. Buffer (20 mM Tris-HCl (pH 7.5), 25 mM NaCl) was added to the solution and after centrifugation, the aqueous layer was removed and lyophilized. This was subsequently run on a Sephadex G-50 gel-filtration column, and the fractions containing Trx were identified by SDS-PAGE and pooled. The protein was dialyzed against water and stored after lyophilization. Activity was monitored by checking its ability to catalyze the DTT-mediated reduction of insulin and the subsequent aggregation of the insulin B chain.⁴⁴

GroEL was purified from a GroE-overproducing strain of *E. coli* harboring the plasmid pOFX6, as described.¹⁶ To remove small, Trp-containing contaminating peptides, an extra step involving passage through a reactive-

red resin was added: the eluted protein was found to be free of impurities, as judged by Trp fluorescence emission. The concentrations of GroEL that refer to the 14-mer were determined using an extinction coefficient of ϵ (0.1%, 1 cm) = 0.2 at 280 nm.¹⁶ A Pharmacia PD-10 column was used to buffer-exchange GroEL into the refolding buffer immediately before use.

Equilibrium unfolding experiments

Equilibrium fluorescence intensities were measured on an SPEX fluorimeter with excitation at 295 nm and the emission collected at 368 nm. The typical protein concentration for a GdnHCl melt was 2 to 4 µM. The refolding buffer used was 30 mM sodium phosphate (pH 7.0), 0.1 M KCl without any reducing agent in order to maintain thioredoxin in its oxidized form under all conditions. All experiments were carried out at 25°C.

Unfolding and refolding kinetics

All rapid kinetic mixing events were carried out using a Biologic SFM-4 stopped-flow module, with a mixing dead-time of 6 ms. Trx (1.5 µM) was unfolded in 4.8 M GdnHCl by mixing 25 µl of 18 µM Trx with 75 µl of refolding buffer and 200 µl of 7.2 M GdnHCl containing refolding buffer. Intrinsic Trp fluorescence emission between 370 and 420 nm was monitored using a band-pass filter, with the excitation set at 295 nm. Refolding of 1.5 µM Trx in 0.3 M GdnHCl was carried out by mixing 25 µl of 18 µM Trx unfolded to equilibrium in 3.6 M GdnHCl, with 275 µl of refolding buffer. In the presence of GroEL, refolding was carried out using increasing concentrations of GroEL in the refolding buffer, keeping the final Trx concentration fixed at 1.5 µM. The small contribution of GroEL to the fluorescence signal, which was mainly due to scattering effects, was determined by mixing 25 µl of unfolding buffer with 275 µl of GroEL-containing refolding buffer, and was subtracted as appropriate from the refolding traces.

Double-jump experiment to monitor the formation of N

Trx (15 µl of 40 µM) unfolded to equilibrium in 3.6 M GdnHCl, was mixed with 165 µl of refolding buffer, so that 3.33 µM Trx commenced folding in 0.3 M GdnHCl. The protein was allowed to refold for various time intervals between 10 and 1000 seconds, before being unfolded at a concentration of 2 µM in 3.2 M GdnHCl by mixing with 120 µl of 8 M GdnHCl. Unfolding was followed using an SPEX fluorimeter (SPEX DM3000), by exciting at 295 nm and collecting the fluorescence emission at 368 nm. In the presence of GroEL, Trx was refolded by diluting it into refolding buffer containing 3.3 µM GroEL.

Double-jump to monitor refolding of transiently unfolded protein

Native Trx was unfolded in 4.8 M GdnHCl at a concentration of 48 µM by mixing 30 µl of 125 µM protein with 48 µl of 7.8 M GdnHCl-containing unfolding buffer. The protein was allowed to unfold for times varying from 1 to 900 seconds before being refolded at a concentration of 3 µM in 0.3 M GdnHCl by mixing 30 µl of this unfolding mix with 450 µl of refolding buffer. To observe the effect of GroEL on the folding of U_{VR} , native Trx was unfolded for ten

seconds in 4.8 M GdnHCl (as described above), and was then refolded at a concentration of 3 μ M in 0.3 M GdnHCl, with the refolding buffer containing 3 μ M (equimolar) GroEL. The two faster phases of fluorescence change were monitored using the Biologic SFM-4 stopped-flow module as described and the slower phases were monitored on the SPEX DM3000 fluorimeter for times varying from 10 to 900 seconds.

Delayed addition of GroEL during Trx refolding

Trx (1.9 μ M) was refolded in 0.38 M GdnHCl by mixing 25 μ l of 18 μ M Trx that had been unfolded to equilibrium in 3.6 M GdnHCl with 210 μ l of refolding buffer. Trx was allowed to refold for periods varying from 20 to 1000 seconds before addition of 65 μ l of 7 μ M GroEL, to give a final concentration of 1.5 μ M GroEL (equimolar to Trx), in 0.3 M GdnHCl. Refolding was followed from the point of addition of GroEL, by exciting at 295 nm and collecting the fluorescence emission at 368 nm.

Data analysis

The dependences of the rapid, medium and slow-phase rates on the GroEL concentrations have been fit to the following equation:³¹

$$k_{\text{obs}} = \frac{1}{2} \left\{ \frac{-K_D - G(k_s - k_g)}{I} + k_s + k_g + \left[\left(\frac{K_D + G(k_s - k_g)}{I} + k_s + k_g \right)^2 - 4 \left(-\frac{(K_D k_s + k_s G)(k_s - k_g)}{I} + k_s k_g \right) \right]^{1/2} \right\} \quad (1)$$

In equation (1), it is assumed that Trx (I) and GroEL (G) form only a 1:1 complex characterized by a dissociation constant K_D . k_s is the rate of free folding of the intermediate in solution and k_g is the rate of folding in the GroEL-bound form.

The dependences of the rapid, medium and slow-phase amplitudes on the GroEL concentrations have been fit to the following equation:

$$S = \frac{(I + K_D + G) - \sqrt{(I + K_D + G)^2 - (4IG)}}{2I} \times (S_{\text{max}} - S_{\text{min}}) + S_{\text{min}} \quad (2)$$

where S is the amplitude, and S_{max} and S_{min} are the maximum and minimum values, respectively.

When N forms from $I_{M,E}$ via $I_{S,E}$, according to a $I_{M,E} \rightarrow I_{S,E} \rightarrow N$ mechanism, the rate of formation of N is given by:

$$N(t) = \left\{ 1 + \frac{1}{k_1 + k_2} [k_2 \exp(-k_1 t) - k_1 \exp(-k_2 t)] \right\} \quad (3)$$

where k_1 and k_2 are the rate constants for the $I_{M,E} \rightarrow I_{S,E}$, and $I_{S,E} \rightarrow N$ reactions, respectively.

Acknowledgments

We thank M. K. Mathew, S. Mayor and R. Varadarajan for discussions; R. Varadarajan for the thioredoxin expression plasmid; and F. N. Zaidi for preliminary experiments. This work was funded by the Tata Institute of Fundamental Research, and by the Department of Science and Technology, J.B.U. is the recipient of a Swarnajayanti Fellowship from the Government of India.

References

- Fenton, W. A., Kashi, Y., Furtak, K. & Horwich, A. L. (1994). Residues in chaperonin GroEL required for polypeptide binding and release. *Nature*, **371**, 614-619.
- Xu, Z., Horwich, A. L. & Sigler, P. B. (1997). The crystal structure of the asymmetric GroEL-GroES-(ADP)₇ chaperonin complex. *Nature*, **388**, 741-750.
- Roseman, A. M., Chen, S., White, H., Braig, K. & Saibil, H. R. (1997). The chaperonin ATPase cycle: mechanism of allosteric switching and movements of substrate-binding domains in GroEL. *Cell*, **87**, 241-251.
- Weissman, J. S., Hohl, C. M., Kovalenko, O., Kashi, Y., Chen, S. & Braig, K., *et al.* (1995). Mechanism of GroEL action: productive release of polypeptide from a sequestered position under GroES. *Cell*, **83**, 577-587.
- Braig, K., Otwinowski, Z., Hedge, R., Boisvert, D. C., Joachimiak, A., Horwich, A. L. & Sigler, P. B. (1994). The crystal structure of the bacterial chaperonin GroEL at 2.8 Å. *Nature*, **371**, 578-586.
- Weissman, J. S., Rye, H. S., Fenton, W. A., Beechem, J. M. & Horwich, A. L. (1996). Characterization of the active intermediate of a GroEL-GroES-mediated protein folding reaction. *Cell*, **84**, 481-490.
- Hayer-Hartl, M. K., Weber, F. & Hartl, F. U. (1996). Mechanism of chaperonin action: GroES binding and release can drive GroEL-mediated protein folding in the absence of ATP-hydrolysis. *EMBO J.* **15**, 6111-6121.
- Rye, H. S., Burston, S. G., Fenton, W. A., Beechem, J. M., Xu, Z., Sigler, P. B. & Horwich, A. L. (1997). Distinct actions of *cis* and *trans* ATP within the double ring of the chaperonin GroEL. *Nature*, **388**, 792-798.
- Rye, H. S., Roseman, A. M., Chen, S., Furtak, K., Fenton, W. A., Saibil, H. R. & Horwich, A. L. (1999). GroEL-GroES cycling: ATP and non-native polypeptide direct alternation of folding-active rings. *Cell*, **97**, 325-338.
- Todd, M. J., Viitanen, P. V. & Lorimer, G. H. (1994). Dynamics of the chaperonin ATPase cycle: implications for facilitated protein folding. *Science*, **265**, 659-666.
- Zahn, R., Spitzfaden, C., Ottiger, M., Wuthrich, K. & Pluckthun, A. (1994). Destabilization of the complete protein secondary structure on binding to the chaperone GroEL. *Nature*, **368**, 261-265.
- Zahn, R., Perrett, S., Stenberg, G. & Fersht, A. R. (1996). Catalysis of amide proton exchange by the molecular chaperones GroEL and SecB. *Science*, **271**, 642-645.
- Walter, S., Lorimer, G. H. & Schmid, F. X. (1996). A thermodynamic coupling mechanism for GroEL-

- mediated unfolding. *Proc. Natl Acad. Sci. USA*, **93**, 9425-9430.
14. Shtilerman, M., Lorimer, G. H. & Englander, S. W. (1999). Chaperonin function: folding by forced unfolding. *Science*, **284**, 822-825.
 15. Coyle, J. E., Texter, F. L., Ashcroft, A. E., Masselos, D., Robinson, C. V. & Radford, S. E. (1999). GroEL accelerates the refolding of hen lysozyme without changing its folding mechanism. *Nature Struct. Biol.* **6**, 683-690.
 16. Bhutani, N. & Udgaonkar, J. B. (2000). A thermodynamic coupling mechanism can explain the GroEL-mediated acceleration of the folding of barstar. *J. Mol. Biol.* **297**, 1037-1044.
 17. Dill, K. A. & Chan, H. S. (1997). From Levinthal to pathways to funnels. *Nature Struct. Biol.* **4**, 10-19.
 18. Fenton, W. A. & Horwich, A. L. (1997). GroEL-mediated protein folding. *Protein Sci.* **6**, 743-760.
 19. Chan, H. S. & Dill, K. A. (1996). A simple model of chaperonin-mediated protein folding. *Proteins: Struct. Funct. Genet.* **24**, 345-351.
 20. Todd, M. J., Lorimer, G. H. & Thirumalai, D. (1996). Chaperonin-facilitated protein folding: optimization of rate and yield by an iterative annealing mechanism. *Proc. Natl Acad. Sci. USA*, **93**, 4030-4035.
 21. Gulukota, K. & Wolynes, P. G. (1994). Statistical mechanics of kinetic proofreading in protein folding *in vivo*. *Proc. Natl Acad. Sci. USA*, **91**, 9292-9296.
 22. Iwakura, M., Jones, B. E., Falzone, C. J. & Matthews, C. R. (1993). Collapse of parallel folding channels in dihydrofolate reductase from *Escherichia coli* by site-directed mutagenesis. *Biochemistry*, **32**, 13566-13574.
 23. Kelley, R. F. & Stellwagen, E. (1984). Conformational transitions of thioredoxin in guanidine hydrochloride. *Biochemistry*, **23**, 5095-5120.
 24. Kelley, R. F., Wilson, J., Bryant, C. & Stellwagen, E. (1986). Effects of guanidine hydrochloride on the refolding kinetics of denatured thioredoxin. *Biochemistry*, **25**, 728-732.
 25. Kelley, R. F., Shalongo, W., Jagannadham, M. V. & Stellwagen, E. (1987). Equilibrium and kinetic measurements of the conformational transition of reduced thioredoxin. *Biochemistry*, **26**, 1406-1411.
 26. Kelley, R. F. & Richards, F. M. (1987). Replacement of proline-76 with alanine eliminates the slowest kinetic phase in thioredoxin folding. *Biochemistry*, **26**, 6765-6774.
 27. Georgescu, R. E., Li, J., Goldberg, M. E., Tasayco, M. L. & Chaffotte, A. F. (1998). Proline isomerization-independent accumulation of an early intermediate and heterogeneity of the folding pathways of a mixed α/β protein, *Escherichia coli* thioredoxin. *Biochemistry*, **37**, 10286-10297.
 28. Katti, S. K., LeMaster, D. M. & Eklund, H. (1990). Crystal structure of thioredoxin from *Escherichia coli* at 1.68 Å resolution. *J. Mol. Biol.* **212**, 167-184.
 29. Stryer, L., Holmgren, A. & Reichard, P. (1967). Thioredoxin. A localized conformational change accompanying reduction of the protein to the sulfhydryl form. *Biochemistry*, **4**, 1016-1020.
 30. Holmgren, A. & Slaby, I. (1979). Thioredoxin C': mechanism of noncovalent complementation and reactions of the refolded complex and the active site containing fragment with thioredoxin reductase. *Biochemistry*, **18**, 5591-5599.
 31. Itzhaki, L. S., Otzen, D. E. & Fersht, A. R. (1995). Nature and consequences of GroEL-protein interactions. *Biochemistry*, **34**, 11581-14587.
 32. Fersht, A. (1999). Measurement and magnitude of individual rate constants. In *Structure and Mechanism in Protein Science*, pp. 143-145, W.H. Freeman & Company, New York.
 33. Corrales, F. & Fersht, A. (1995). The folding of GroEL-bound barnase as a model for chaperonin-mediated protein folding. *Proc. Natl Acad. Sci. USA*, **92**, 5326-5330.
 34. Gray, T. E. & Fersht, A. R. (1993). Refolding of barnase in the presence of GroE. *J. Mol. Biol.* **232**, 1197-1207.
 35. Tsurupa, G. P., Ikura, T., Makio, T. & Kuwajima, K. (1998). Refolding kinetics of staphylococcal nuclease and its mutants in the presence of the chaperonin GroEL. *J. Mol. Biol.* **277**, 733-745.
 36. Katsumata, K., Okazaki, A. & Kuwajima, K. (1996). Effect of GroEL on the re-folding kinetics of α -lactalbumin. *J. Mol. Biol.* **258**, 827-838.
 37. Sparrer, H., Lilie, H. & Buchner, J. (1996). Dynamics of the GroEL-protein complex: effects of nucleotides and folding mutants. *J. Mol. Biol.* **258**, 74-87.
 38. Mendoza, J. A., Lorimer, G. H. & Horowitz, P. M. (1991). Intermediates in the chaperonin-assisted refolding of rhodanese are trapped at low temperature and show a small stoichiometry. *J. Biol. Chem.* **266**, 16973-16976.
 39. Goldberg, M. S., Zhang, J., Sondek, S., Matthews, C. R., Fox, R. O. & Horwich, A. L. (1997). Native-like structure of a protein-folding intermediate bound to the chaperonin GroEL. *Proc. Natl Acad. Sci. USA*, **94**, 1080-1085.
 40. Ikura, T., Tsurupa, G. P. & Kuwajima, K. (1997). Kinetic folding and cis/trans prolyl isomerization of staphylococcal nuclease. A study by stopped-flow absorption, stopped-flow circular dichroism, and molecular dynamics simulations. *Biochemistry*, **36**, 6529-6538.
 41. Maki, K., Ikura, T., Hayano, T., Takahashi, N. & Kuwajima, K. (1999). Effects of proline mutations on the folding of staphylococcal nuclease. *Biochemistry*, **38**, 2213-2223.
 42. Ghoshal, A. K., Swaminathan, C. P., Thomas, C. J., Suroliya, A. & Varadarajan, R. (1999). Thermodynamic and kinetic analysis of the *Escherichia coli* thioredoxin-C' fragment complementation system. *Biochem. J.* **339**, 721-727.
 43. Ames, G. F., Prody, C. & Kustu, S. (1984). Simple, rapid, and quantitative release of periplasmic proteins by chloroform. *J. Bacteriol.* **160**, 1181-1183.
 44. Holmgren, A. (1979). Thioredoxin catalyzes the reduction of insulin disulphides by Dithiothreitol and dihydrolipoamide. *J. Biol. Chem.* **254**, 9627-9632.
 45. Agashe, V. R. & Udgaonkar, J. B. (1995). Thermodynamics of denaturation of barstar: evidence for cold denaturation and evaluation of the interaction with guanidine hydrochloride. *Biochemistry*, **34**, 3286-3299.

Edited by C. R. Matthews

(Received 26 June 2001; received in revised form 16 October 2001; accepted 17 October 2001)